THE JOURNAL OF BIOLOGICAL CHEMISTRY VOL. 288, NO. 6, pp. 4368–4377, February 8, 2013

Pyruvate:Ferredoxin Oxidoreductase Is Coupled to Light-independent Hydrogen Production in *Chlamydomonas reinhardtii*[*]

Received for publication, October 22, 2012, and in revised form, December 18, 2012 Published, JBC Papers in Press, December 20, 2012, DOI 10.1074/jbc.M112.429985

Jens Noth, Danuta Krawietz, Anja Hemschemeier, and Thomas Happe[1]

From the Ruhr Universität Bochum, Fakultät für Biologie und Biotechnologie, AG Photobiotechnologie, 44801 Bochum, Germany

Background: The pathway(s) of light-independent H_2 production in green algae are yet unknown.
Results: Pyruvate:ferredoxin oxidoreductase PFR1 and [Fe-Fe]-hydrogenase HYDA1 of *Chlamydomonas* can be coupled for pyruvate-dependent H_2 production.
Conclusion: H_2 production by green algae in the dark is similar to bacterial PFOR-dependent fermentation.
Significance: Understanding the fermentation metabolism of green algae allows insights into plastid bioenergetic pathways.

In anaerobiosis, the green alga *Chlamydomonas reinhardtii* evolves molecular hydrogen (H_2) as one of several fermentation products. H_2 is generated mostly by the [Fe-Fe]-hydrogenase HYDA1, which uses plant type ferredoxin PETF/FDX1 (PETF) as an electron donor. Dark fermentation of the alga is mainly of the mixed acid type, because formate, ethanol, and acetate are generated by a pyruvate:formate lyase pathway similar to *Escherichia coli*. However, *C. reinhardtii* also possesses the pyruvate:ferredoxin oxidoreductase PFR1, which, like pyruvate:formate lyase and HYDA1, is localized in the chloroplast. PFR1 has long been suggested to be responsible for the low but significant H_2 accumulation in the dark because the catalytic mechanism of pyruvate:ferredoxin oxidoreductase involves the reduction of ferredoxin. With the aim of proving the biochemical feasibility of the postulated reaction, we have heterologously expressed the *PFR1* gene in *E. coli*. Purified recombinant PFR1 is able to transfer electrons from pyruvate to HYDA1, using the ferredoxins PETF and FDX2 as electron carriers. The high reactivity of PFR1 toward oxaloacetate indicates that *in vivo*, fermentation might also be coupled to an anaerobically active glyoxylate cycle. Our results suggest that *C. reinhardtii* employs a clostridial type H_2 production pathway in the dark, especially because *C. reinhardtii* PFR1 was also able to allow H_2 evolution in reaction mixtures containing *Clostridium acetobutylicum* 2[4Fe-4S]-ferredoxin and [Fe-Fe]-hydrogenase HYDA.

Chlamydomonas reinhardtii is a photoautotrophic eukaryote that is equipped with a repertoire of fermentative enzymes allowing the cells to perform a mixed acid type fermentation (1–4). Of special interest for biotechnological applications is the capability of the cells to generate molecular hydrogen (H_2) in the absence of oxygen (O_2) (5). H_2 is generated by a highly efficient hydrogenase of the [Fe-Fe] type, HYDA1 (6–8), which, despite its extreme sensitivity toward O_2 (9–11), is located in the chloroplast (6). The natural electron donor of HYDA1 is the photosynthetic ferredoxin PETF (7, 12), and the highest rates of H_2 evolution are observed in the light (4, 13). However, the cells have to be adapted to dark anaerobic conditions to induce hydrogenase activity (7, 14). Upon the shift to illumination, H_2 production is only transient, because the hydrogenase enzymes are inactivated by photosynthetically generated O_2 (15), and assimilatory photosynthetic electron sinks, the Calvin cycle above all, are reactivated (16, 17). However, a sustained H_2 metabolism in illuminated *C. reinhardtii* cells is induced by sulfur deprivation (18). Sulfur deficiency results in a strongly reduced photosystem 2 activity, mainly because of photo-damage and inadequate recycling of the D1 core subunit of photosystem 2 (19–21). Hence, incubated in sealed flasks, sulfur-deficient algae establish hypoxic conditions despite illumination, because O_2 evolution rates drop below respiratory O_2 consumption (18). Anerobiosis elicits hydrogenase gene expression (22, 23) and allows the O_2-intolerant enzyme to be active. However, only the diminution of assimilatory electron sinks caused by cessation of cell division (18, 21) allows sustained and relatively high H_2 evolution rates (17). Electrons for photosynthetic H_2 production originate from residual photosystem 2 activity (24–26) but also from nonphotochemical plastoquinone reduction via plastidic NAD(P)H:plastoquinone oxidoreductase NDA2 (27–29). Electrons for this photosystem 2-independent, so-called indirect pathway result from oxidative starch and possibly protein degradation (18, 24, 26). It is generally accepted that in sulfur-deprived *C. reinhardtii* cells, H_2 generation serves as an alternative electron sink, allowing photosynthetic electron transport and thus energy generation to continue while preventing an over-reduction of the photosynthetic machinery (18, 25).

H_2 production in nutrient-deficient green algae, however, is not the only pathway allowing the cells to maintain an energy and redox balance. Rather, the cells accumulate formate and ethanol simultaneously (30–32). The excretion of nongaseous fermentation products prevails in anaerobic *Chlamydomonas* cells in the dark (4). The generation of formate, ethanol, and acetate in a ratio of 2:1:1 in dark-incubated algae resembles

* This work was supported by grants from the Deutsches Zentrum für Luft- und Raumfahrt (ModuLES) and the Volkswagen Foundation (LigH2t) (to T. H.).

[1] To whom correspondence should be addressed: Ruhr Universität Bochum, Fakultät für Biologie und Biotechnologie, AG Photobiotechnologie, Universitätsstr. 150, 44801 Bochum, Germany. Tel.: 49-234-32-27026; Fax: 49-234-32-14322; E-mail: thomas.happe@rub.de.

mixed acid fermentation of prokaryotes like the enterobacterium *Escherichia coli* (33). The presence of a pyruvate:formate lyase (PFL1), catalyzing the thioclastic cleavage of pyruvate to formate and acetyl-CoA in the eukaryotic alga, was therefore proposed (34) and genetically and biochemically proven (2, 30, 35). Because *C. reinhardtii* does not contain genes for a formate-hydrogen lyase complex that is responsible for formate-dependent H_2 generation in fermenting *E. coli* (33), light-independent H_2 production in the green alga was proposed to result from pyruvate:ferredoxin oxidoreductase (PFOR)[2] activity (36). A *Chlamydomonas* PFOR (PFR1) was identified on the genetic (2) and protein levels, and the protein is located in the chloroplast of the cells (37, 38). PFOR enzymes oxidatively decarboxylate pyruvate to yield acetyl-CoA and CO_2, simultaneously transferring electrons to flavodoxin or ferredoxin (39). Thereby, ferredoxin reduction by plastidic *C. reinhardtii* PFR1 might couple fermentative pyruvate catabolism to H_2 generation in a way typical for strict anaerobic bacteria of the genus *Clostridium* (40–43).

In this study we show that *C. reinhardtii* PFR1 heterologously produced in *E. coli* is active in pyruvate- and oxaloacetate-dependent methyl viologen reduction. Moreover, PFR1 enables methyl viologen- or ferredoxin-dependent H_2 production by isolated *Chlamydomonas* HYDA1, which proves that the long postulated pathway of dark H_2 generation in the green alga is biochemically possible.

EXPERIMENTAL PROCEDURES

Organisms and Growth Conditions—E. coli strain DH5α MCR (Novagen) was used for cloning procedures. Heterologous expression of *C. reinhardtii* PFR1 and ferredoxin encoding cDNAs was done in *E. coli* BL21 (DE3) Δ*iscR* (44, 45). *E. coli* strains were grown according to standard procedures as described before (30). *Clostridium acetobutylicum* ATCC 824 was used for heterologous synthesis of *C. reinhardtii* HYDA1 and homologous expression of *C. acetobutylicum* [Fe-Fe]-hydrogenase HYDA and ferredoxin CAC0303.

C. reinhardtii strain CC124 (137c, *mt− nit1− nit2−*) was grown in Tris acetate-phosphate (TAP) medium (46) on a shaker with bottom-up illumination of 100 μmol of photons·m^{-2}·s^{-1} at 20 °C. For determination of *in vivo* H_2 production rates in the light or in the dark, *C. reinhardtii* cultures were grown until they reached a chlorophyll (Chl) content of 15 μg·ml^{-1}, harvested by mild centrifugation (2,000 × *g*, 3 min, 20 °C), and resuspended in fresh TAP medium to reach a final Chl concentration of 110 μg·ml^{-1}. The cell suspension was transferred to a shaded flask and purged with nitrogen gas for 4 h. *In vitro* hydrogenase activity was determined as described before (47) to ensure the anaerobic induction. Afterward, 2-ml aliquots of the cell culture were withdrawn using a syringe and transferred to sealed and O_2-free head space bottles. Half of the withdrawn 2-ml aliquots were incubated in the dark and half in the light (100 μmol of photons·m^{-2}·s^{-1}). The H_2 amount in the head space was analyzed after various time points of incubation by gas chromatography as reported previously (35).

Cloning of C. reinhardtii PFR1 cDNA—Total RNA of anaerobic algal cells was isolated according to Philipps *et al.* 2011 (35), and cDNA was synthesized after DNase digestion (Turbo DNAfree kit; Ambion) using Superscript II reverse transcriptase (Invitrogen) according to the manufacturer's instructions. The *PFR1* coding region was amplified from this cDNA with hot start *Pfu* DNA polymerase (Stratagene) using oligonucleotides 5′-TT**GGATCC**CCCGCCGCTGCTGGCCGCGCCACCAACG-3′ and 5′-TA**GATATC**ACGTCCTTCTATTCTAGAGTGGCCGCCGCAGCCGCTCT-3′. The bold letters indicate restriction sites for BamHI and EcoRV used for cloning. The forward oligonucleotide was generated in a way that the protein encoded by the cDNA would lack the putative chloroplast target sequence indicated by the first V*X*A amino acid motif typical for cleavage of *Chlamydomonas* chloroplast targeting sequences (48). The sequence was ligated with vector pASK-IBA37 (IBA GmbH) via BamHI and EcoRV restriction sites. This resulted in construct pIBA37_PFR1, allowing a tightly regulated expression via the anhydrotetracycline inducible *tet* promoter and in recombinant PFR1 enzyme equipped with an N-terminal His_6 tag.

Heterologous Production and Purification of His-tagged Recombinant PFR1 and Other Proteins—E. coli BL21 (DE3) Δ*iscR* (44) was transformed with vector pIBA37_PFR1 by electroporation (49). Precultures were grown shaking in 200 ml of LB medium at 37 °C overnight and used to inoculate four 2-liter flasks, each containing 500 ml of Vogel-Bonner minimal medium (50) with 100 μg·ml^{-1} ampicillin, 0.2 μM of the O_2 indicator resazurin, and 50 μM thiamine hydrochloride. As soon as the cultures had reached an A_{600} of 0.6 after growth at 37 °C, 5 g of glucose·l^{-1} was added to the medium, and the cell suspensions were transferred to a 2-liter bottle. Expression of the *PFR1* cDNA was induced by adding 0.2 μg·ml^{-1} anhydrotetracycline. The flasks were sealed air tight and incubated at 8 °C overnight. Then the suspension was transferred to centrifugation flasks in an anaerobic tent (Toepfer LabSystems), and the cells were harvested by centrifugation (20 min at 7,500 × *g*, 4 °C). All further steps were also conducted under strictly anaerobic conditions (1% H_2, 99% N_2) in the anaerobic tent. The *E. coli* cell pellet was resuspended in O_2-free buffer (100 mM Tris-HCl, pH 8.0, 10% (v/v) glycerol), and the cells were lysed by sonication (five times for 30 s; output, 25; Branson Sonifier 250). Cell debris was removed by centrifugation (60 min, 200,000 × *g*, 4 °C). The soluble fraction was filtered through sterile filters (pore size, 0.2 μm; Sarstedt AG & Co.) and loaded on a 4-ml gravity flow nickel-nitrilotriacetic acid fast flow column pre-equilibrated with 100 mM Tris-HCl, pH 8.0, 10 mM imidazole, and 0.5 mM thiamine pyrophosphate (TPP). Removal of unspecifically binding proteins was obtained by washing the column with the above mentioned buffer containing increased concentrations of imidazole (40-ml steps with 10 and 20 mM imidazole). His-tagged PFR1 was eluted in 1.2-ml steps using 10 ml of buffer containing 100 mM imidazole. Protein concentration of the main fraction was determined spectrophotometrically (NanoDrop; Peqlab) at λ = 280 nm, and this protein solution was used for further analysis. The size and purity of the eluted protein fractions were analyzed by denatur-

[2] The abbreviations used are: PFOR, pyruvate:ferredoxin oxidoreductase; Chl, chlorophyll; TPP, thiamine pyrophosphate; PETF, ferredoxin PETF/FDX1.

ating SDS-PAGE according to standard techniques (51). PFR1 activity tests were conducted immediately after purification.

Heterologous production of *C. reinhardtii* [Fe-Fe]-hydrogenase HYDA1, as well as homologous production of HYDA in *C. acetobutylicum* and subsequent purification via Strep-tag II was done as described before (52, 53). Recombinant *Chlamydomonas* [2Fe2S]-ferredoxins PETF and FDX5 were obtained as published previously (12, 54). *C. reinhardtii* FDX2 was produced accordingly by amplifying the *FDX2* coding region without the N-terminal transit peptide encoding sequence using oligonucleotides 5′-ATGGTA**GGTCTC**AGCGCCACTTTA-AGGTCACGTTTAAGACC-3′ and 5′-ATGGTA**GGTCTC**A-TATCAGAGCTTGGACTCCTGGTCGGT-3′ (BsaI restriction sites are indicated by bold letters). The *C. acetobutylicum* ferredoxin CAC0303 encoding region was amplified from the *E. coli* expression vector pET21c0303 (55) using hot start *Pfu* DNA polymerase (Stratagene) with oligonucleotides 5′-GAA-**GGATCC**GCATATAAAATAACAGACGCTTGTG-3′ and 5′-AAGC**GGCGCC**ACGGAGCTCGAATTCT-3′. The bold letters mark the BamHI and EheI restriction sites used for ligation with the clostridial expression vector pThydA_{CR1}-C-tag after excision of its insert (52). All further steps (transformation and cultivation of *C. acetobutylicum*, as well as protein purification) were done as described before (53).

PFR1 Activity Assays Using Methyl Viologen as Artificial Electron Acceptor—The enzymatic activity of recombinant *C. reinhardtii* PFR1 was determined by following the reduction of methyl viologen spectrophotometrically at $\lambda = 604$ nm (56) using a 96-well plate reader (Beckmann, Paradigm 1113) operated in an anaerobic tent and connected to a PC running multimode analysis software. The molar extinction coefficient of methyl viologen used was $\epsilon_{604} = 13.6\ \text{mM}^{-1}\ \text{cm}^{-1}$ (57). The standard reaction mixture contained 1.4 μM recombinant PFR1, 100 mM Tris-HCl, pH 8.0, 10 mM sodium pyruvate, 2 mM sodium CoA, 5 mM TPP, 10 mM methyl viologen, and 16 mM dithioerythritol in a final volume of 100 μl. The reaction was started by adding PFR1 and conducted at room temperature. Absorbance was measured every 30 s until saturation was reached. The value obtained after 6 min, which was in the late linear phase, was used for determining activity. Kinetics were performed varying the concentration of one substrate while keeping the concentrations of all other substrates constant and saturating. The K_m and V_{max} values were determined in each reaction and calculated using GraphPad Prism® software.

In Vitro Reconstitution of PFR1-coupled H_2 Production—For analyzing the H_2 producing capacity of [Fe-Fe]-hydrogenases upon electron delivery by PFR1-catalyzed ferredoxin reduction, recombinant enzymes and proteins were mixed in various combinations. The standard reaction mixture contained 0.7 μM recombinant PFR1, 40 μM ferredoxin, 0.01 μM hydrogenase, 10 mM sodium pyruvate, 2 mM sodium CoA, 5 mM TPP, and 16 mM dithioerythritol in 200 μl of 100 mM potassium-phosphate buffer, pH 6.8. The reactions were carried out in sealed 2-ml reaction vessels. Before incubation, the reaction mixtures were purged with argon for 3 min to reset the system. After incubation for 30 min at 37 °C in a shaking water bath, 400 μl of the head space were injected in a gas chromatograph (GC-2010 (Shimadzu), equipped with a PLOT fused silica coating molsieve column (5 Å, 10 m × 0.32 mm) from Varian) to determine the H_2 concentration.

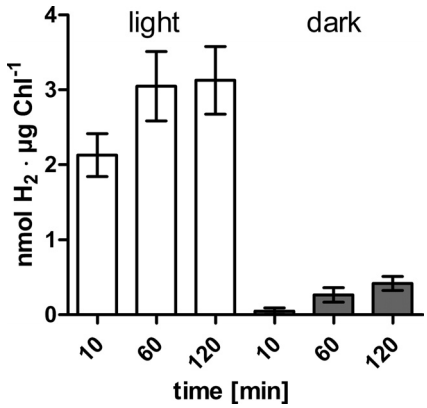

FIGURE 1. ***In vivo* H_2 evolution rates of *C. reinhardtii* cultures in the light or in the dark.** Concentrated cell suspensions were flushed with nitrogen for 4 h until they had reached an *in vitro* hydrogenase activity of 109 ± 18 nmol of $H_2 \cdot \mu g\ Chl^{-1} \cdot h^{-1}$. Then culture aliquots were withdrawn, transferred to gas tight head space bottles, and incubated in the light (*white bars*) or the dark (*gray bars*) until the indicated time points before determining the H_2 concentration of the head space by gas chromatography. The results shown are the mean values from three independent experiments carried out as technical duplicates. The *error bars* indicate the standard deviation.

RESULTS

Recombinant C. reinhardtii PFR1 Has Typical PFOR Activity—As described in the introduction, *in vivo* H_2 production in *C. reinhardtii* is higher in the light, because electrons are provided by photosynthetic activity. We compared the light-dependent and -independent H_2 evolution rates of anaerobically adapted *Chlamydomonas* cell suspensions in a setup moderately modified from those reported before (as in Ref. 35, for example) (Fig. 1). In cells transferred from anaerobic conditions in the dark to illumination, H_2 accumulated to 2.13 nmol of $H_2 \cdot \mu g\ Chl^{-1}$ within the first 10 min, whereas cells kept in the dark produced only 0.05 nmol of $H_2 \cdot \mu g\ Chl^{-1}$ in the same time period (Fig. 1). In the following 50 min, the cells exposed to light produced additional 0.92 nmol of $H_2 \cdot \mu g\ Chl^{-1}$ (plus 43.2%) and shaded cells generated 0.22 nmol of $H_2 \cdot \mu g\ Chl^{-1}$ (plus 437.5%). In both illuminated and dark-incubated *C. reinhardtii* cell suspensions, H_2 generation rates slowed down in the following hour, because the former evolved 0.078 nmol of $H_2 \cdot \mu g\ Chl^{-1}$ and the latter evolved 0.152 nmol of $H_2 \cdot \mu g\ Chl^{-1}$ (Fig. 1). To analyze whether the low but significant H_2 production in dark-adapted algae might be driven by pyruvate oxidation via PFOR activity, *Chlamydomonas* PFR1 was heterologously produced.

The annotated gene models of the *C. reinhardtii PFR1* gene have changed considerably from the first *Chlamydomonas* genome version to the most recent annotation on Phytozome v8.0, *C. reinhardtii* v5.3. Although most parts of the primary sequences are the same in the newest gene models (Cre11.g473950.t1.1 and g1910.t2 on Phytozome v8.0, *C. reinhardtii* v4.3 and v5.3, respectively, and au5.g2553_t1 and SKA_Chlre2_kg.scaffold_62000019 on JGIv4), a region starting at position 940 in the Cre11.g473950.t1.1 protein model is highly variable. We aligned all available PFR1 models, as well as the sequence translated from the *PFR1* cDNA amplified in this study with bacterial enzymes and concluded that the cDNA and

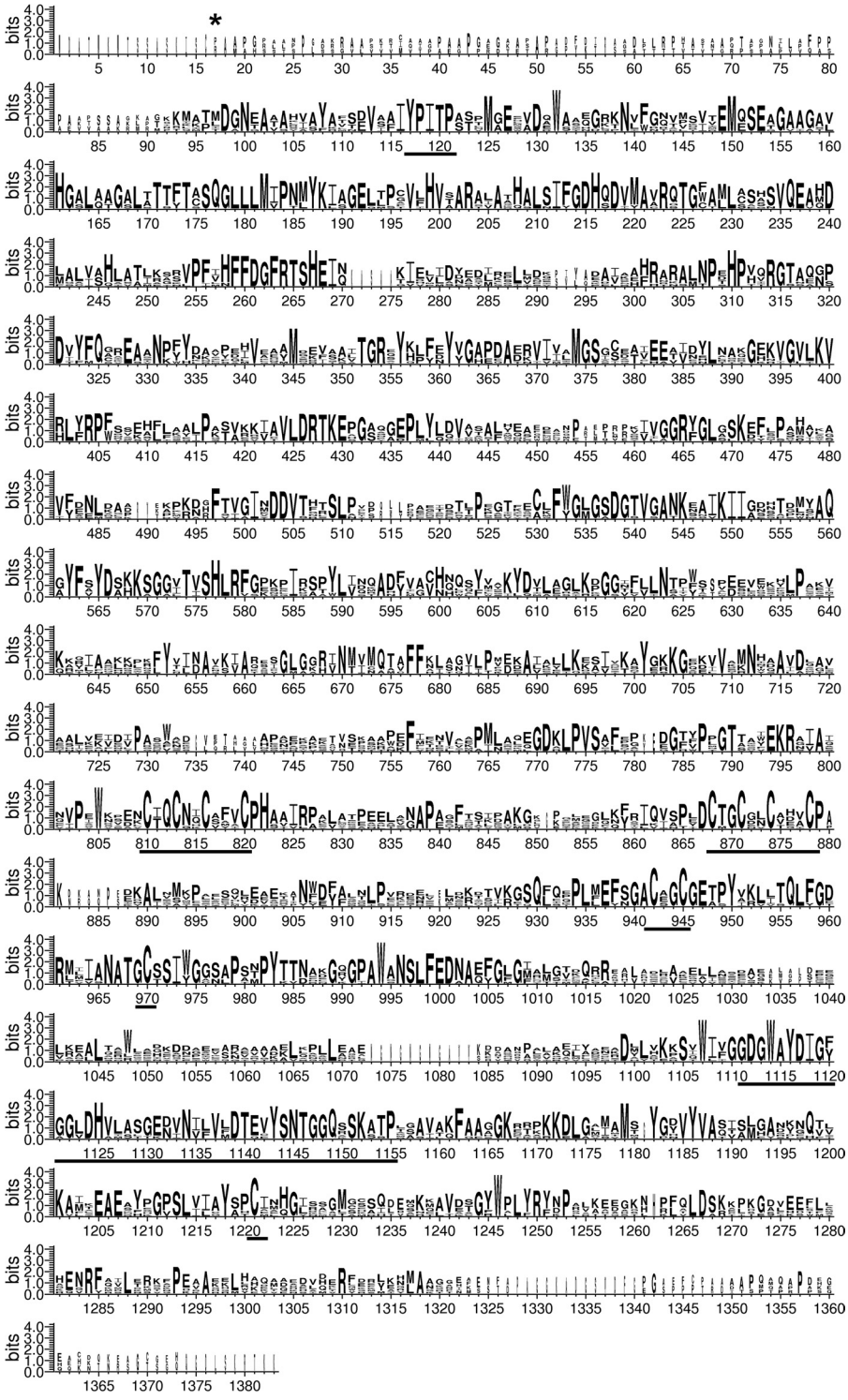

FIGURE 2. **Stacked polypeptide alignment of pyruvate:ferredoxin oxidoreductase primary sequences.** Eight PFOR sequences were used for an alignment using ClustalW2 and WebLogo 3 (89, 90). These sequences were *C. reinhardtii* PFR1 derived from the cDNA obtained in this study, *Volvox carteri f. nagariensis* (Phytozome v8.0, *V. carteri* Vocar20008508m), *Chlorella variabilis* (GenBank™ EFN55341.1), *C. acetobutylicum* PFO (GenBank™ NP_348846.1), *Clostridium pasteurianum* (GenBank™ AAD55756.1), *Desulfovibrio africanus* POR (GenBank™ CAA70873.1), *E. coli* YdbK (GenBank™ YP_002999180.1), and *Synechococcus* sp. PCC.7002 NifJ (GenBank™ ACA99434.1). The conserved YPITP substrate-binding site (58), as well as three [4Fe-4S]-cluster coordinating motifs and the region homologous to TPP-binding (59, 91) sites, are *underlined*. Note that the third [4Fe-4S]-cluster-binding site is atypical and consists of the C*XX*C motif at positions 942–945 and two separated cysteines at positions 970 and 1221 (60, 61). The first amino acid of recombinant PFR1 is marked by an *asterisk*.

protein sequences, respectively, obtained here are correct (*i.e.*, amino acids AKKWVLFCARLLTQ starting at position 940 in Cre11.g473950.t1.1 are actually missing). Therefore, we used the protein sequence deduced from our cDNA for the alignment shown in Fig. 2. The alignments revealed that the *C. reinhardtii* PFR1 polypeptide sequence contains all sequence motifs known to be essential for PFOR enzyme activity (marked in Fig. 2). It features an N-terminal conserved 2-oxoacid-bind-

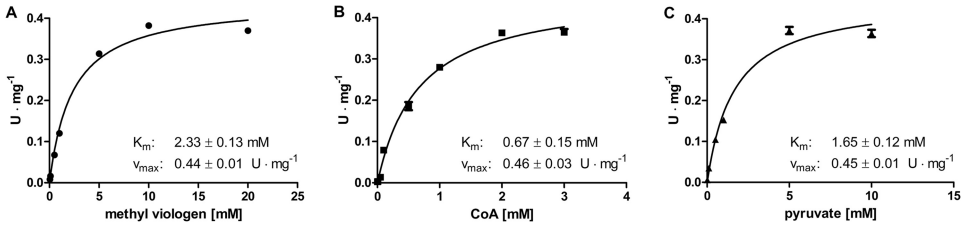

FIGURE 3. **Kinetic parameters of recombinant *C. reinhardtii* PFR1 heterologously produced in *E. coli* and purified via His-tag affinity chromatography.** Enzymatic activity was determined following the reduction of methyl viologen spectrophotometrically in 100-μl reaction mixtures containing 1.4 μM PFR1, 5 mM TPP, 16 mM dithioerythritol in 100 mM Tris-HCl, pH 8. The K_m values of the individual substrates were determined in the presence of 2 mM CoA and 10 mM pyruvate (*A*, methyl viologen), 10 mM methyl viologen and 10 mM pyruvate (*B*, CoA), or 2 mM CoA and 10 mM methyl viologen (*C*, pyruvate). Each kinetic was analyzed from two independent PFR1 preparations as technical duplicates. The K_m and V_{max} values were calculated using GraphPad Prism® software. The graphs show the mean values, and the *error bars* indicate the standard deviation.

ing site (YPITP) (58), a C-terminal TPP-binding site (59), and three [4Fe-4S]-cluster-binding signatures, two of which are typical for 2[4Fe-4S]-ferredoxins and one of which is atypical (60, 61) (Fig. 2). The comparisons with bacterial enzymes revealed that the *C. reinhardtii* PFR1 sequence contains an N-terminal extension that is not homologous to other PFOR proteins. Because PFR1 was shown to be localized in the chloroplast (37), we assumed that the first V*X*A amino acid motif (starting at position 24 of Cre11.g473950.t1.1) might represent a chloroplast targeting sequence cleavage site (48). Therefore, we excluded the respective region encoding these first 24 residues from the cDNA used for heterologous production of PFR1.

After heterologous expression of the truncated *PFR1* cDNA in *E. coli* and subsequent purification of the His-tagged protein via nickel-nitrilotriacetic acid chromatography, a protein of the expected size (144 kDa) could be eluted. Activity assays using pyruvate and CoA as substrates and methyl viologen as artificial electron acceptor resulted in a specific activity of 0.45 ± 0.01 units·mg^{-1} (1 unit was defined as the conversion of 1 μmol of pyruvate or CoA and the reduction of 2 μmol of methyl viologen, respectively, per minute) (Fig. 3). The K_m values obtained for methyl viologen, CoA, and pyruvate in this assay were 2.3, 0.7, and 1.7 mM, respectively (Fig. 3).

Chlamydomonas PFR1 Allows Pyruvate-dependent H_2 Production—To analyze whether PFR1-catalyzed pyruvate oxidation would allow H_2 production by *C. reinhardtii* HYDA1, reconstitution assays were performed in which various combinations of electron carriers (methyl viologen, and ferredoxins) were mixed. The combination of recombinant PFR1 and *C. reinhardtii* HYDA1 in the presence of pyruvate, CoA, and methyl viologen as artificial electron carrier resulted in a H_2 production rate of 400 ± 66 nmol of H_2·min^{-1}·mg PFR1^{-1}, which was only slightly higher than the rate obtained with *Chlamydomonas* ferredoxin PETF (Fig. 4*A*; 338 ± 32 nmol of H_2·min^{-1}·mg PFR1^{-1}). The K_m value of PFR1 for PETF was determined as 2.4 ± 0.34 μM (Fig. 4*B*), which is considerably lower than the K_m value of HYDA1 for PETF (20–30 μM) (7, 12). We also examined whether two further ferredoxins, FDX2 and FDX5, would allow PFR1-dependent H_2 evolution. *FDX2* (62) and especially *FDX5* transcripts and FDX5 protein (54, 63, 64) have been shown to accumulate in anaerobic *Chlamydomonas* cells, which makes them candidates for being involved in pathways specific for anaerobiosis. Furthermore, both ferredoxin isoforms are localized in the plastid (54, 62) together with HYDA1 and PFR1. Using FDX2 as electron carrier, a PFR1-dependent H_2 evolution rate of 287 ± 15 nmol of H_2·min^{-1}·mg PFR1^{-1} could be observed, whereas no activity was determined using FDX5 (Fig. 4*A*). Notably, recombinant *C. reinhardtii* PFR1 also allowed H_2 generation of *C. acetobutylicum* HYDA in the presence of the clostridial ferredoxin CAC0303 in a rate of 118 ± 35 nmol of H_2·min^{-1}·mg PFR1^{-1} (Fig. 4*A*).

Using the amount of recombinant *C. reinhardtii* HYDA1 enzyme as a basis, the PFR1- and methyl viologen-mediated H_2 production rates (80 ± 13 μmol of H_2·min^{-1}·mg HYDA1^{-1}) were only 16% of those determined with sodium diothionite-reduced methyl viologen (516 ± 42 μmol of H_2·min^{-1}·mg HYDA1^{-1}; Table 1). However, in the presence of PETF as the electron carrier, the reaction driven by 0.7 μM PFR1 reached 42% of the reaction in which sodium diothionite served as chemical electron donor (68 ± 7 *versus* 160 ± 17 μmol of H_2·min^{-1}·mg HYDA1^{-1}; Table 1). In this reaction mixture, 0.7 μM PFR1 was close to saturation because the rates obtained using 0.35 μM PFR1 were 61 ± 9, and those in assays containing 0.9 μM PFR1 were 72 ± 8 μmol of H_2·min^{-1}·mg HYDA1^{-1}.

PFR1 Is Able to Use Oxaloacetate, but Not α-Ketoglutarate as a Substrate—Some bacterial PFOR enzymes have been reported to be able to oxidize various substrates such as 2-oxoacid:ferredoxin oxidoreductase from *Sulfolobus* species strain 7 or *Sulfolobus solfataricus* P1 (58, 65), whereas others such as PFOR from *E. coli* can only oxidize pyruvate (66). We examined the methyl viologen reducing activity of *C. reinhardtii* PFR1 in the presence of oxaloacetate and α-ketoglutarate. When oxaloacetate was included in the reaction mixture, a specific activity of 0.26 ± 0.03 U·mg^{-1} was observed, but no methyl viologen reduction could be detected using α-ketoglutarate (Fig. 5*A*). In a reconstitution assay using the same substrates but using the electron carrier PETF and the [Fe-Fe]-hydrogenase HYDA1 to examine substrate-dependent H_2 evolution, oxaloacetate was almost as suitable as pyruvate, whereas no H_2 production could be observed in the presence of α-ketoglutarate (Fig. 5*B*).

DISCUSSION

C. reinhardtii has long been known for its complex mixed acid fermentative metabolism, which has more similarities to fermentation of bacteria or strictly anaerobic protists than to plant or animal anaerobic pathways (1, 2, 4, 34). In addition to PFL1, which is mainly known from enterobacteria such as *E. coli* (33), a cDNA encoding pyruvate:ferredoxin oxidoreduc-

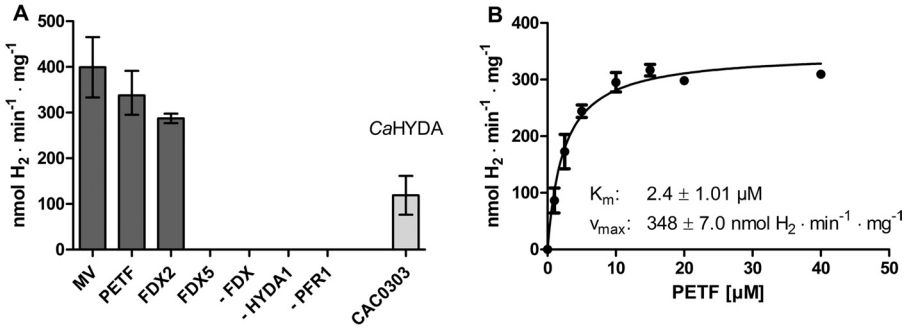

FIGURE 4. **H_2 generation in reconstitution assays of recombinant *C. reinhardtii* PFR1 and [Fe-Fe]-hydrogenases.** *A*, each reaction contained PFR1 (0.7 μM) and 0.01 μM HYDA1 of *C. reinhardtii* (except one reaction, which contained *C. acetobutylicum* ferredoxin (CAC0303) and [Fe-Fe]-hydrogenase HYDA, indicated by the label *CaHYDA*), 10 mM pyruvate, and 2 mM CoA in 100 mM potassium phosphate buffer, pH 6.8. Electron carriers were applied as indicated below the *x* axis (10 mM methyl viologen (*MV*), 40 μM of the *Chlamydomonas* ferredoxins PETF, FDX2, or FDX5, or 40 μM clostridial ferredoxin CAC0303). The reaction mixtures were incubated for 30 min at 37 °C before analyzing the amount of H_2 in the gas phase. As controls, reaction mixtures were analyzed that lacked one of the enzymes or proteins indicated by a *dash*. *B*, the dependence of PFR1-coupled H_2 generation on PETF concentration was determined using *C. reinhardtii* HYDA1 in reaction mixtures as described for *A* and the indicated concentrations of PETF. The values and standard deviations shown in all of the experiments are from three independent PFR1 preparations, and the H_2 production rate was related to mg of PFR1 enzyme. The *error bars* indicate the standard deviation.

TABLE 1

H_2 evolution rates of *C. reinhardtii* HYDA1 using electrons provided by sodium dithionite (NaDT) or pyruvate oxidation via PFR1 related to the amounts of hydrogenase protein

All of the reactions contained 100 mM potassium phosphate buffer and 0.01 μM *C. reinhardtii* HYDA1. PFR1-containing reactions included 10 mM pyruvate and 2 mM CoA. The values shown were derived from three independent PFR1 and HYDA1 preparations ± standard deviation.

Reaction components	$H_2 \cdot min^{-1} \cdot mg\ HYDA1^{-1}$
	µmol
100 mM NaDT, 10 mM methyl viologen	516 ± 42
50 mM NaDT, 40 μM PETF	160 ± 17
0.7 μM PFR1, 10 mM methyl viologen	80 ± 13
0.7 μM PFR1, 40 μM PETF	68 ± 7

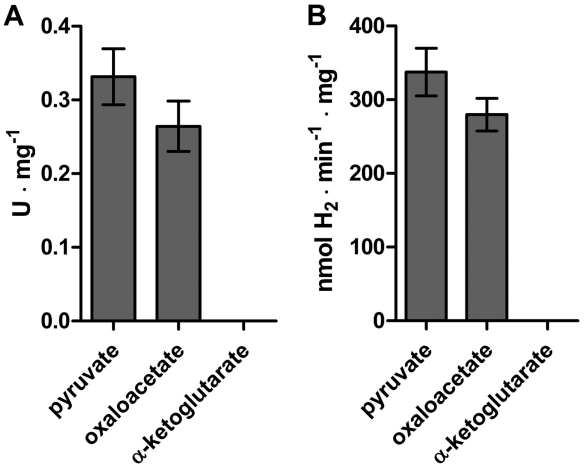

FIGURE 5. **Substrate specificity of *C. reinhardtii* PFR1.** The capacity of PFR1 to reduce methyl viologen (*A*) and to drive H_2 evolution by *C. reinhardtii* HYDA1 (*B*) using oxaloacetate or α-ketoglutarate was examined. The reaction mixtures contained 10 mM pyruvate, oxaloacetate, or α-ketoglutarate and 2 mM CoA in 100 mM potassium phosphate buffer, pH 6.8, and additionally 1.4 μM PFR1 and 10 mM methyl viologen (*A*) or 0.7 μM PFR1, 40 μM PETF, and 0.01 μM HYDA1 (*B*). *A*, methyl viologen reduction was determined spectrophotometrically. *B*, H_2 evolution rates were determined by gas chromatography as described in the legend of Fig. 4. The results shown are the means and standard deviations from two independent experiments carried out as technical duplicates.

tase was identified in *C. reinhardtii* (2) and shown to accumulate in anaerobic algal cells (30, 63). PFR1 was proposed to be involved in dark H_2 production by *C. reinhardtii* (36, 63) in analogy to fermentative H_2 production in clostridiae (40, 42, 67) or anaerobic hydrogenosome containing protists (68, 69). This model was supported by the phenotype of a *Chlamydomonas pfl1* mutant strain, which showed higher yields of ethanol, CO_2, and H_2 generation in the dark (35). The fermentative pattern of the mutant was interpreted in a way that the absence of PFL1 would result in higher pyruvate supply to PFR1, which reduces ferredoxin upon oxidative decarboxylation of pyruvate to acetyl-CoA and CO_2. In contrast, further allelic *pfl1* mutants reported recently do not exhibit higher dark H_2 generation in a different experimental setup (70). Other metabolic pathways providing electrons for H_2 generation in the dark were also discussed, such as ferredoxin reduction by FNR in analogy to the pathways allowing sulfate assimilation in the roots of higher plants (71).

In this study we show that PFR1-driven H_2 production is biochemically plausible, because recombinant *C. reinhardtii* PFR1 is able to allow H_2 generation by isolated [Fe-Fe]-hydrogenases. Although these results cannot prove that this reaction occurs in living *Chlamydomonas* cells, they indicate that the PFR1-dependent pyruvate to H_2 pathway can be operable *in vivo* (Fig. 6). The biochemical properties of the purified PFR1 protein are similar to PFOR enzymes isolated and characterized from other organisms regarding pyruvate- and CoA-dependent methyl viologen reduction (72, 73). The K_m values for pyruvate and methyl viologen were in the range of the K_m values determined for other PFOR enzymes, whereas the K_m for CoA was higher (74–76). Also, the specific activity of our PFR1 preparations were at the lower range when compared with other PFOR enzymes (74, 77, 78). This might support the physiological data obtained so far, which all speak for PFL1 being the major fermentative enzyme in *C. reinhardtii* wild type cultures (4, 30, 35). However, we cannot exclude that the protein solution contained inactive PFR1 enzymes. We observed a marked instability of the enzyme, despite its isolation and examination under strictly anaerobic conditions sufficient for the analysis of the extremely O_2-sensitive [Fe-Fe]-hydrogenase of *C. reinhardtii* (9–11). Instability of isolated PFOR enzymes has been reported before (79), and besides destruction by O_2 (73, 80), loss of the TPP factor has been proposed to be one reason for this phenomenon (75).

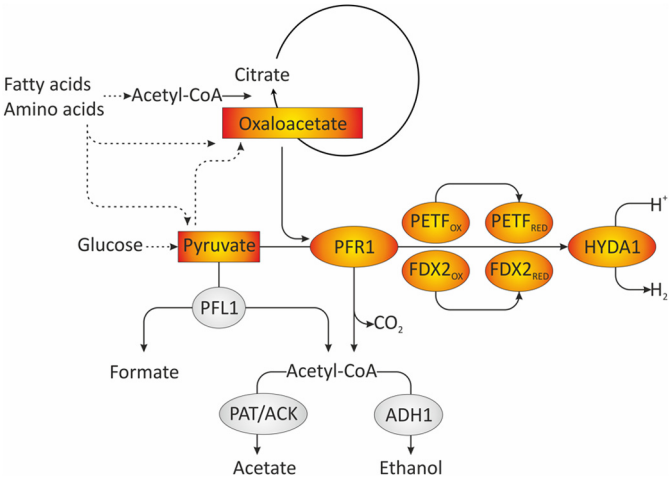

FIGURE 6. **Model of fermentative pathways involved in dark anaerobic H_2 production in *C. reinhardtii*.** In the wild type, PFL1 is the major fermentative enzyme in short term anaerobiosis and cleaves pyruvate into formate and acetyl-CoA. The latter can be reduced to ethanol via bifunctional acetaldehyde-alcohol dehydrogenase (ADH1) (92) or converted to acetate via phosphotransacetylase and acetate kinase (*PAT/ACK*). In addition to PFL1, PFR1 is capable of pyruvate oxidation. In a *pfl1* mutant or in long term anaerobiosis, pyruvate oxidation might be preferably catalyzed by PFR1. PFR1 transfers electrons to ferredoxins and thereby allows H_2 generation via the [Fe-Fe]-hydrogenase. In addition to pyruvate, PFR1 is able to use oxaloacetate as a substrate. This might link the oxidation of other substrates such as fatty acids or amino acids to fermentative H_2 production, possibly via an anaerobically operating glyoxylate cycle or parts thereof.

In reaction mixtures combining PFR1 with *C. reinhardtii* HYDA1 and ferredoxin PETF, which is the most suitable redox partner for HYDA1 known so far (12), a pyruvate-dependent H_2 production could be observed, showing that the postulated reaction is possible. Notably, PFR1-driven H_2 generation via PETF was only 2.5-fold lower than H_2 generation using sodium dithionite-reduced PETF as an electron donor for HYDA1. This indicates that the capacity of PFR1-coupled H_2 production is quite high, despite the low specific activity of PFR1. We assume that both the low K_m value of PFR1 for PETF and the high specific activity of HYDA1 contribute to the high efficiency of the coupled system. The low rates of *in vivo* H_2 evolution in dark-incubated algal cells are therefore probably limited by PFR1 substrate supply rather than by PFR1 activity.

PFR1-mediated H_2 production by HYDA1 was also possible using FDX2 as an electron carrier (Fig. 6), and the rates obtained were only moderately lower than with PETF. Notably, FDX2 lacks one phenylalanine residue that, in PETF, is essential for proper interaction with HYDA1 (12, 81). The capability of HYDA1 to generate H_2 using FDX2 as an electron donor in the PFR1-driven system might therefore indicate a different interaction mechanism. FDX2 was suggested to be specifically involved in nitrite reduction. The protein can hardly be detected in *C. reinhardtii* cells incubated in ammonium-containing medium but accumulates in cells growing on nitrate and allows a higher catalytic activity of *Chlamydomonas* nitrite reductase than PETF (62). However, because FDX2 was also as efficient as PETF for FNR catalytic activity and even better regarding affinity (62), FDX2 might in general be used for reactions that can also employ PETF.

The results obtained with FDX2 indicated that the electron transfer reaction coupling PFR1 and HYDA1 might be different from the other electron delivering reactions analyzed so far. Therefore we analyzed whether FDX5 was able to shuttle electrons between PFR1 and HYDA1, although FDX5 is unable to drive H_2 generation activity upon artificial reduction (54). The *FDX5* gene is strongly induced upon anaerobiosis (54, 63) but also in copper-deficient *C. reinhardtii* cells (62, 64, 82). *FDX5* is regulated by CRR1 (the copper response regulator 1) under both conditions (64). Notably, it was shown recently that the *HYDA1* gene is also activated by the absence of copper (82) and partially regulated by CRR1 (83). Although a connection between FDX5 and HYDA1 might be suggested from these findings, the data presented here confirm that a direct metabolic interaction does not take place.

PFOR-mediated H_2 generation is central to anaerobic energy generation in several strict anaerobes such as amitochondriates (69) and clostridiae (67). Notably, *C. reinhardtii* was able to allow *C. acetobutylicum* HYDA activity in the presence of clostridial 2[4Fe-4S]-ferredoxin. This indicates that PFR1 kept the basic features of the evolutionary old PFOR protein (68, 84), despite the fact that *C. reinhardtii* and clostridial PFOR sequences were calculated to be evolutionary distant (85). A similar promiscuity regarding redox partners was observed for other PFOR enzymes, such as *Clostridium thermoaceticum* (74) and *Rhodobacter capsulatus* PFORs (86).

Recombinant *C. reinhardtii* PFR1 had methyl viologen reducing and H_2 driving activity also in the presence of oxaloacetate as substrate, whereas α-ketoglutarate did not result in measurable activity. Both metabolites are intermediates of the TCA cycle, whereas the branch via α-ketoglutarate and succinyl-CoA is absent in the glyoxylate cycle. An anaerobically operating glyoxylate cycle is active in the alga (87), and the oxidation of malate was suggested to contribute to H_2 photoproduction (88). Pyruvate and oxaloacetate are furthermore end products of the catabolism of several amino acids. It might be assumed that oxaloacetate degradation by PFR1 supports the anaerobic operation of the glyoxylate cycle or parts thereof (Fig. 6). The physiological role of PFR1 in fermenting *C. reinhardtii* cells might therefore become important during long term fermentation. A 2:1:1 ratio of formate:ethanol:acetate production observed in algae after 4–6 h of anaerobiosis (4, 34, 35) is typical for pyruvate:formate lyase activity. However, formate production only prevails in the first hours of anaerobiosis, whereas ethanol and especially CO_2 generation rates increase thereafter, simultaneously to a slowdown of starch degradation (34). Although speculative, a scenario might be envisioned in which PFL1 is mostly responsible for short term fermentation using starch and glucose, respectively, as substrate. In long term anaerobiosis, PFR1 activity would allow *Chlamydomonas* to utilize acetyl-CoA derived from fatty acids and end products of amino acid catabolism as energy sources (Fig. 6). Furthermore, the coupling to the hydrogenase is a means to dispose of electrons via the nontoxic and highly diffusible H_2 molecule.

Acknowledgments—We are thankful for the gift of pET21c0303 from Laurence Girbal (Laboratoire d'Ingénierie des Systèmes Biologiques et des Procédés, Toulouse, France). We also thank Annika Brünje and Simone Schmidt for technical support during cloning of CAC0303 and *FDX2.*

REFERENCES

1. Hemschemeier, A., and Happe, T. (2005) The exceptional photofermentative hydrogen metabolism of the green alga *Chlamydomonas reinhardtii*. *Biochem. Soc. Trans.* **33,** 39–41
2. Atteia, A., van Lis, R., Gelius-Dietrich, G., Adrait, A., Garin, J., Joyard, J., Rolland, N., and Martin, W. (2006) Pyruvate formate-lyase and a novel route of eukaryotic ATP synthesis in *Chlamydomonas* mitochondria. *J. Biol. Chem.* **281,** 9909–9918
3. Atteia, A., van Lis, R., Tielens, A. G., and Martin, W. F. (2013) Anaerobic energy metabolism in unicellular photosynthetic eukaryotes. *Biochim. Biophys. Acta* **1827,** 210–223
4. Gfeller, R. P., and Gibbs, M. (1984) Fermentative metabolism of *Chlamydomonas reinhardtii*. I. Analysis of fermentative products from starch in dark and light. *Plant Physiol.* **75,** 212–218
5. Hemschemeier, A., and Happe, T. (2011) Alternative photosynthetic electron transport pathways during anaerobiosis in the green alga *Chlamydomonas reinhardtii*. *Biochim. Biophys. Acta* **1807,** 919–926
6. Happe, T., Mosler, B., and Naber, J. D. (1994) Induction, localization and metal content of hydrogenase in the green alga *Chlamydomonas reinhardtii*. *Eur. J. Biochem.* **222,** 769–774
7. Happe, T., and Naber, J. D. (1993) Isolation, characterization and N-terminal amino acid sequence of hydrogenase from the green alga *Chlamydomonas reinhardtii*. *Eur. J. Biochem.* **214,** 475–481
8. Kamp, C., Silakov, A., Winkler, M., Reijerse, E. J., Lubitz, W., and Happe, T. (2008) Isolation and first EPR characterization of the [FeFe]-hydrogenases from green algae. *Biochim. Biophys. Acta* **1777,** 410–416
9. Goldet, G., Brandmayr, C., Stripp, S. T., Happe, T., Cavazza, C., Fontecilla-Camps, J. C., and Armstrong, F. A. (2009) Electrochemical kinetic investigations of the reactions of [FeFe]-hydrogenases with carbon monoxide and oxygen. Comparing the importance of gas tunnels and active-site electronic/redox effects. *J. Am. Chem. Soc.* **131,** 14979–14989
10. Lambertz, C., Leidel, N., Havelius, K. G., Noth, J., Chernev, P., Winkler, M., Happe, T., and Haumann, M. (2011) O_2 reactions at the six-iron active site (H-cluster) in [FeFe]-hydrogenase. *J. Biol. Chem.* **286,** 40614–40623
11. Stripp, S. T., Goldet, G., Brandmayr, C., Sanganas, O., Vincent, K. A., Haumann, M., Armstrong, F. A., and Happe, T. (2009) How oxygen attacks [FeFe] hydrogenases from photosynthetic organisms. *Proc. Natl. Acad. Sci. U.S.A.* **106,** 17331–17336
12. Winkler, M., Kuhlgert, S., Hippler, M., and Happe, T. (2009) Characterization of the key step for light-driven hydrogen evolution in green algae. *J. Biol. Chem.* **284,** 36620–36627
13. Stuart, T. S., and Gaffron, H. (1972) The mechanism of hydrogen photoproduction by several algae. *Planta* **106,** 101–112
14. Gaffron, H., and Rubin, J. (1942) Fermentative and photochemical production of hydrogen in algae. *J. Gen. Physiol.* **26,** 219–240
15. Ghirardi, M. L., Togasaki, R. K., and Seibert, M. (1997) Oxygen sensitivity of algal H_2-production. *Appl. Biochem. Biotechnol.* **63–65,** 141–151
16. Cinco, R. M., MacInnis, J. M., and Greenbaum, E. (1993) The role of carbon dioxide in light-activated hydrogen production by *Chlamydomonas reinhardtii*. *Photosynth. Res.* **38,** 27–33
17. Rühle, T., Hemschemeier, A., Melis, A., and Happe, T. (2008) A novel screening protocol for the isolation of hydrogen producing *Chlamydomonas reinhardtii* strains. *BMC Plant Biol.* **8,** 107
18. Melis, A., Zhang, L., Forestier, M., Ghirardi, M. L., and Seibert, M. (2000) Sustained photobiological hydrogen gas production upon reversible inactivation of oxygen evolution in the green alga *Chlamydomonas reinhardtii*. *Plant Physiol.* **122,** 127–136
19. Wykoff, D. D., Davies, J. P., Melis, A., and Grossman, A. R. (1998) The regulation of photosynthetic electron transport during nutrient deprivation in *Chlamydomonas reinhardtii*. *Plant Physiol.* **117,** 129–139
20. Chen, H. C., Newton, A. J., and Melis, A. (2005) Role of SulP, a nuclear-encoded chloroplast sulfate permease, in sulfate transport and H_2 evolution in *Chlamydomonas reinhardtii*. *Photosynth. Res.* **84,** 289–296
21. Davies, J. P., Yildiz, F. H., and Grossman, A. (1996) Sac1, a putative regulator that is critical for survival of *Chlamydomonas reinhardtii* during sulfur deprivation. *EMBO J.* **15,** 2150–2159
22. Happe, T., and Kaminski, A. (2002) Differential regulation of the Fe-hydrogenase during anaerobic adaptation in the green alga *Chlamydomonas reinhardtii*. *Eur. J. Biochem.* **269,** 1022–1032
23. Forestier, M., King, P., Zhang, L., Posewitz, M., Schwarzer, S., Happe, T., Ghirardi, M. L., and Seibert, M. (2003) Expression of two [Fe]-hydrogenases in *Chlamydomonas reinhardtii* under anaerobic conditions. *Eur. J. Biochem.* **270,** 2750–2758
24. Fouchard, S., Hemschemeier, A., Caruana, A., Pruvost, J., Legrand, J., Happe, T., Peltier, G., and Cournac, L. (2005) Autotrophic and mixotrophic hydrogen photoproduction in sulfur-deprived *Chlamydomonas* cells. *Appl. Environ. Microbiol.* **71,** 6199–6205
25. Hemschemeier, A., Fouchard, S., Cournac, L., Peltier, G., and Happe, T. (2008) Hydrogen production by *Chlamydomonas reinhardtii*. An elaborate interplay of electron sources and sinks. *Planta* **227,** 397–407
26. Chochois, V., Dauvillée, D., Beyly, A., Tolleter, D., Cuiné, S., Timpano, H., Ball, S., Cournac, L., and Peltier, G. (2009) Hydrogen production in *Chlamydomonas*. Photosystem II-dependent and -independent pathways differ in their requirement for starch metabolism. *Plant Physiol.* **151,** 631–640
27. Desplats, C., Mus, F., Cuiné, S., Billon, E., Cournac, L., and Peltier, G. (2009) Characterization of Nda2, a plastoquinone-reducing type II NAD(P)H dehydrogenase in *Chlamydomonas* chloroplasts. *J. Biol. Chem.* **284,** 4148–4157
28. Jans, F., Mignolet, E., Houyoux, P. A., Cardol, P., Ghysels, B., Cuiné, S., Cournac, L., Peltier, G., Remacle, C., and Franck, F. (2008) A type II NAD(P)H dehydrogenase mediates light-independent plastoquinone reduction in the chloroplast of *Chlamydomonas*. *Proc. Natl. Acad. Sci. U.S.A.* **105,** 20546–20551
29. Mignolet, E., Lecler, R., Ghysels, B., Remacle, C., and Franck, F. (2012) Function of the chloroplastic NAD(P)H dehydrogenase Nda2 for H_2 photoproduction in sulphur-deprived *Chlamydomonas reinhardtii*. *J. Biotechnol.* **162,** 81–88
30. Hemschemeier, A., Jacobs, J., and Happe, T. (2008) Biochemical and physiological characterization of the pyruvate formate-lyase Pfl1 of *Chlamydomonas reinhardtii*, a typically bacterial enzyme in a eukaryotic alga. *Eukaryot. Cell* **7,** 518–526
31. Philipps, G., Happe, T., and Hemschemeier, A. (2012) Nitrogen deprivation results in photosynthetic hydrogen production in *Chlamydomonas reinhardtii*. *Planta* **235,** 729–745
32. Winkler, M., Heil, B., Heil, B., and Happe, T. (2002) Isolation and molecular characterization of the [Fe]-hydrogenase from the unicellular green alga *Chlorella fusca*. *Biochim. Biophys. Acta* **1576,** 330–334
33. Sawers, R. G. (2005) Formate and its role in hydrogen production in *Escherichia coli*. *Biochem. Soc. Trans.* **33,** 42–46
34. Kreuzberg, K. (1984) Starch fermentation via a formate producing pathway in *Chlamydomonas reinhardii*, *Chlorogonium elongatum* and *Chlorella fusca*. *Physiol. Plant.* **61,** 87–94
35. Philipps, G., Krawietz, D., Hemschemeier, A., and Happe, T. (2011) A pyruvate formate lyase-deficient *Chlamydomonas reinhardtii* strain provides evidence for a link between fermentation and hydrogen production in green algae. *Plant J.* **66,** 330–340
36. Grossman, A. R., Catalanotti, C., Yang, W., Dubini, A., Magneschi, L., Subramanian, V., Posewitz, M. C., and Seibert, M. (2011) Multiple facets of anoxic metabolism and hydrogen production in the unicellular green alga *Chlamydomonas reinhardtii*. *New Phytol.* **190,** 279–288
37. Terashima, M., Specht, M., Naumann, B., and Hippler, M. (2010) Characterizing the anaerobic response of *Chlamydomonas reinhardtii* by quantitative proteomics. *Mol. Cell. Proteomics* **9,** 1514–1532
38. Terashima, M., Specht, M., and Hippler, M. (2011) The chloroplast proteome. A survey from the *Chlamydomonas reinhardtii* perspective with a focus on distinctive features. *Curr. Genet.* **57,** 151–168
39. Ragsdale, S. W. (2003) Pyruvate ferredoxin oxidoreductase and its radical intermediate. *Chem. Rev.* **103,** 2333–2346
40. Carere, C. R., Kalia, V., Sparling, R., Cicek, N., and Levin, D. B. (2008) Pyruvate catabolism and hydrogen synthesis pathway genes of *Clostridium thermocellum* ATCC 27405. *Indian J. Microbiol.* **48,** 252–266
41. Kim, B. H., Bellows, P., Datta, R., and Zeikus, J. G. (1984) Control of carbon and electron flow in *Clostridium acetobutylicum* fermentations. Utilization of carbon monoxide to inhibit hydrogen production and to enhance

butanol yields. *Appl. Environ. Microbiol.* **48,** 764–770
42. Calusinska, M., Happe, T., Joris, B., and Wilmotte, A. (2010) The surprising diversity of clostridial hydrogenases. A comparative genomic perspective. *Microbiology* **156,** 1575–1588
43. Demuez, M., Cournac, L., Guerrini, O., Soucaille, P., and Girbal, L. (2007) Complete activity profile of *Clostridium acetobutylicum* [FeFe]-hydrogenase and kinetic parameters for endogenous redox partners. *FEMS Microbiol. Lett.* **275,** 113–121
44. Akhtar, M. K., and Jones, P. R. (2008) Deletion of *iscR* stimulates recombinant clostridial Fe-Fe hydrogenase activity and H_2-accumulation in *Escherichia coli* BL21(DE3). *Appl. Microbiol. Biotechnol.* **78,** 853–862
45. Schwartz, C. J., Giel, J. L., Patschkowski, T., Luther, C., Ruzicka, F. J., Beinert, H., and Kiley, P. J. (2001) IscR, an Fe-S cluster-containing transcription factor, represses expression of *Escherichia coli* genes encoding Fe-S cluster assembly proteins. *Proc. Natl. Acad. Sci. U.S.A.* **98,** 14895–14900
46. Harris, E. H. (1989) *The Chlamydomonas Sourcebook: A Comprehensive Guide to Biology and Laboratory Use*, Academic Press, San Diego
47. Hemschemeier, A., Melis, A., and Happe, T. (2009) Analytical approaches to photobiological hydrogen production in unicellular green algae. *Photosynth. Res.* **102,** 523–540
48. Franzén, L. G., Rochaix, J. D., and von Heijne, G. (1990) Chloroplast transit peptides from the green alga *Chlamydomonas reinhardtii* share features with both mitochondrial and higher plant chloroplast presequences. *FEBS Lett.* **260,** 165–168
49. Sambrook, J., and Russell, D. W. (2006) Transformation of *E. coli* by Electroporation. *CSH Protoc.* **2006,** pii
50. Vogel, H. J., and Bonner, D. M. (1956) Acetylornithinase of *Escherichia coli*. Partial purification and some properties. *J. Biol. Chem.* **218,** 97–106
51. Sambrook, J., Fritsch, E. F., and Maniatis, T. (1989) *Molecular Cloning: A Laboratory Manual*, 2nd Ed., Cold Spring Harbor Laboratory Press, Cold Spring Harbor, NY
52. Girbal, L., von Abendroth, G., Winkler, M., Benton, P. M., Meynial-Salles, I., Croux, C., Peters, J. W., Happe, T., and Soucaille, P. (2005) Homologous and heterologous overexpression in *Clostridium acetobutylicum* and characterization of purified clostridial and algal Fe-only hydrogenases with high specific activities. *Appl. Environ. Microbiol.* **71,** 2777–2781
53. von Abendroth, G., Stripp, S., Silakov, A., Croux, C., Soucaille, P., Girbal, L., and Happe, T. (2008) Optimized over-expression of [FeFe] hydrogenases with high specific activity in *Clostridium acetobutylicum*. *Int. J. Hydrogen Energy* **33,** 6076–6081
54. Jacobs, J., Pudollek, S., Hemschemeier, A., and Happe, T. (2009) A novel, anaerobically induced ferredoxin in *Chlamydomonas reinhardtii*. *FEBS Lett.* **583,** 325–329
55. Guerrini, O., Burlat, B., Léger, C., Guigliarelli, B., Soucaille, P., and Girbal, L. (2008) Characterization of two 2[4Fe4S] ferredoxins from *Clostridium acetobutylicum*. *Curr. Microbiol.* **56,** 261–267
56. Zeikus, J. G., Fuchs, G., Kenealy, W., and Thauer, R. K. (1977) Oxidoreductases involved in cell carbon synthesis of *Methanobacterium thermoautotrophicum*. *J. Bacteriol.* **132,** 604–613
57. Mayhew, S. G. (1978) The redox potential of dithionite and SO_2 from equilibrium reactions with flavodoxins, methyl viologen and hydrogen plus hydrogenase. *Eur. J. Biochem.* **85,** 535–547
58. Fukuda, E., Kino, H., Matsuzawa, H., and Wakagi, T. (2001) Role of a highly conserved YPITP motif in 2-oxoacid:ferredoxin oxidoreductase. Heterologous expression of the gene from *Sulfolobus* sp. strain 7, and characterization of the recombinant and variant enzymes. *Eur. J. Biochem.* **268,** 5639–5646
59. Hawkins, C. F., Borges, A., and Perham, R. N. (1989) A common structural motif in thiamin pyrophosphate-binding enzymes. *FEBS Lett.* **255,** 77–82
60. Chabrière, E., Charon, M. H., Volbeda, A., Pieulle, L., Hatchikian, E. C., and Fontecilla-Camps, J. C. (1999) Crystal structures of the key anaerobic enzyme pyruvate:ferredoxin oxidoreductase, free and in complex with pyruvate. *Nat. Struct. Biol.* **6,** 182–190
61. Pieulle, L., Magro, V., and Hatchikian, E. C. (1997) Isolation and analysis of the gene encoding the pyruvate-ferredoxin oxidoreductase of *Desulfovibrio africanus*, production of the recombinant enzyme in *Escherichia coli*, and effect of carboxy-terminal deletions on its stability. *J. Bacteriol.* **179,** 5684–5692
62. Terauchi, A. M., Lu, S. F., Zaffagnini, M., Tappa, S., Hirasawa, M., Tripathy, J. N., Knaff, D. B., Farmer, P. J., Lemaire, S. D., Hase, T., and Merchant, S. S. (2009) Pattern of expression and substrate specificity of chloroplast ferredoxins from *Chlamydomonas reinhardtii*. *J. Biol. Chem.* **284,** 25867–25878
63. Mus, F., Dubini, A., Seibert, M., Posewitz, M. C., and Grossman, A. R. (2007) Anaerobic acclimation in *Chlamydomonas reinhardtii*. Anoxic gene expression, hydrogenase induction, and metabolic pathways. *J. Biol. Chem.* **282,** 25475–25486
64. Lambertz, C., Hemschemeier, A., and Happe, T. (2010) Anaerobic expression of the ferredoxin-encoding *FDX5* gene of *Chlamydomonas reinhardtii* is regulated by the Crr1 transcription factor. *Eukaryot. Cell* **9,** 1747–1754
65. Park, Y. J., Yoo, C. B., Choi, S. Y., and Lee, H. B. (2006) Purifications and characterizations of a ferredoxin and its related 2-oxoacid:ferredoxin oxidoreductase from the hyperthermophilic archaeon, *Sulfolobus solfataricus* P1. *J. Biochem. Mol. Biol.* **39,** 46–54
66. Blaschkowski, H. P., Neuer, G., Ludwig-Festl, M., and Knappe, J. (1982) Routes of flavodoxin and ferredoxin reduction in *Escherichia coli*. CoA-acylating pyruvate:flavodoxin and NADPH: flavodoxin oxidoreductases participating in the activation of pyruvate formate-lyase. *Eur. J. Biochem.* **123,** 563–569
67. Carpenter, C. E., Reddy, D. S., and Cornforth, D. P. (1987) Inactivation of clostridial ferredoxin and pyruvate-ferredoxin oxidoreductase by sodium nitrite. *Appl. Environ. Microbiol.* **53,** 549–552
68. Horner, D. S., Hirt, R. P., and Embley, T. M. (1999) A single eubacterial origin of eukaryotic pyruvate:ferredoxin oxidoreductase genes. Implications for the evolution of anaerobic eukaryotes. *Mol. Biol. Evol.* **16,** 1280–1291
69. Hackstein, J. H., Akhmanova, A., Boxma, B., Harhangi, H. R., and Voncken, F. G. (1999) Hydrogenosomes. Eukaryotic adaptations to anaerobic environments. *Trends Microbiol.* **7,** 441–447
70. Catalanotti, C., Dubini, A., Subramanian, V., Yang, W., Magneschi, L., Mus, F., Seibert, M., Posewitz, M. C., and Grossman, A. R. (2012) Altered fermentative metabolism in *Chlamydomonas reinhardtii* mutants lacking pyruvate formate lyase and both pyruvate formate lyase and alcohol dehydrogenase. *Plant Cell* **24,** 692–707
71. Yonekura-Sakakibara, K., Onda, Y., Ashikari, T., Tanaka, Y., Kusumi, T., and Hase, T. (2000) Analysis of reductant supply systems for ferredoxin-dependent sulfite reductase in photosynthetic and nonphotosynthetic organs of maize. *Plant Physiol.* **122,** 887–894
72. Pieulle, L., Guigliarelli, B., Asso, M., Dole, F., Bernadac, A., and Hatchikian, E. C. (1995) Isolation and characterization of the pyruvate-ferredoxin oxidoreductase from the sulfate-reducing bacterium *Desulfovibrio africanus*. *Biochim. Biophys. Acta* **1250,** 49–59
73. Pineda, E., Encalada, R., Rodríguez-Zavala, J. S., Olivos-García, A., Moreno-Sánchez, R., and Saavedra, E. (2010) Pyruvate:ferredoxin oxidoreductase and bifunctional aldehyde-alcohol dehydrogenase are essential for energy metabolism under oxidative stress in *Entamoeba histolytica*. *FEBS J.* **277,** 3382–3395
74. Furdui, C., and Ragsdale, S. W. (2000) The role of pyruvate ferredoxin oxidoreductase in pyruvate synthesis during autotrophic growth by the Wood-Ljungdahl pathway. *J. Biol. Chem.* **275,** 28494–28499
75. Uyeda, K., and Rabinowitz, J. C. (1971) Pyruvate-ferredoxin oxidoreductase. 3. Purification and properties of the enzyme. *J. Biol. Chem.* **246,** 3111–3119
76. Menon, S., and Ragsdale, S. W. (1997) Mechanism of the *Clostridium thermoaceticum* pyruvate:ferredoxin oxidoreductase. Evidence for the common catalytic intermediacy of the hydroxyethylthiamine pyropyrosphate radical. *Biochemistry* **36,** 8484–8494
77. Lin, W. C., Yang, Y. L., and Whitman, W. B. (2003) The anabolic pyruvate oxidoreductase from *Methanococcus maripaludis*. *Arch. Microbiol.* **179,** 444–456
78. Blamey, J. M., and Adams, M. W. (1993) Purification and characterization of pyruvate ferredoxin oxidoreductase from the hyperthermophilic archaeon *Pyrococcus furiosus*. *Biochim. Biophys. Acta* **1161,** 19–27
79. Meinecke, B., Bertram, J., and Gottschalk, G. (1989) Purification and char-

acterization of the pyruvate-ferredoxin oxidoreductase from *Clostridium acetobutylicum*. *Arch. Microbiol.* **152,** 244–250
80. Cavazza, C., Contreras-Martel, C., Pieulle, L., Chabrière, E., Hatchikian, E. C., and Fontecilla-Camps, J. C. (2006) Flexibility of thiamine diphosphate revealed by kinetic crystallographic studies of the reaction of pyruvate-ferredoxin oxidoreductase with pyruvate. *Structure* **14,** 217–224
81. Winkler, M., Hemschemeier, A., Jacobs, J., Stripp, S., and Happe, T. (2010) Multiple ferredoxin isoforms in *Chlamydomonas reinhardtii*. Their role under stress conditions and biotechnological implications. *Eur. J. Cell Biol.* **89,** 998–1004
82. Castruita, M., Casero, D., Karpowicz, S. J., Kropat, J., Vieler, A., Hsieh, S. I., Yan, W., Cokus, S., Loo, J. A., Benning, C., Pellegrini, M., and Merchant, S. S. (2011) Systems biology approach in *Chlamydomonas* reveals connections between copper nutrition and multiple metabolic steps. *Plant Cell* **23,** 1273–1292
83. Pape, M., Lambertz, C., Happe, T., and Hemschemeier, A. (2012) Differential expression of the *Chlamydomonas* [FeFe]-hydrogenase-encoding *HYDA1* gene is regulated by the copper response regulator 1. *Plant Physiol.* **159,** 1700–1712
84. Embley, T. M., van der Giezen, M., Horner, D. S., Dyal, P. L., Bell, S., and Foster, P. G. (2003) Hydrogenosomes, mitochondria and early eukaryotic evolution. *IUBMB Life* **55,** 387–395
85. Hug, L. A., Stechmann, A., and Roger, A. J. (2010) Phylogenetic distributions and histories of proteins involved in anaerobic pyruvate metabolism in eukaryotes. *Mol. Biol. Evol.* **27,** 311–324
86. Yakunin, A. F., and Hallenbeck, P. C. (1998) Purification and characterization of pyruvate oxidoreductase from the photosynthetic bacterium *Rhodobacter capsulatus*. *Biochim. Biophys. Acta* **1409,** 39–49
87. Gibbs, M., Gfeller, R. P., and Chen, C. (1986) Fermentative metabolism of *Chlamydomonas reinhardii*. III. Photoassimilation of acetate. *Plant Physiol.* **82,** 160–166
88. Willeford, K. O., and Gibbs, M. (1989) Localization of the enzymes involved in the photoevolution of H_2 from acetate in *Chlamydomonas reinhardtii*. *Plant Physiol.* **90,** 788–791
89. Larkin, M. A., Blackshields, G., Brown, N. P., Chenna, R., McGettigan, P. A., McWilliam, H., Valentin, F., Wallace, I. M., Wilm, A., Lopez, R., Thompson, J. D., Gibson, T. J., and Higgins, D. G. (2007) Clustal W and Clustal X version 2.0. *Bioinformatics* **23,** 2947–2948
90. Crooks, G. E., Hon, G., Chandonia, J. M., and Brenner, S. E. (2004) WebLogo. A sequence logo generator. *Genome Res.* **14,** 1188–1190
91. Muller, Y. A., Lindqvist, Y., Furey, W., Schulz, G. E., Jordan, F., and Schneider, G. (1993) A thiamin diphosphate binding fold revealed by comparison of the crystal structures of transketolase, pyruvate oxidase and pyruvate decarboxylase. *Structure* **1,** 95–103
92. Magneschi, L., Catalanotti, C., Subramanian, V., Dubini, A., Yang, W., Mus, F., Posewitz, M. C., Seibert, M., Perata, P., and Grossman, A. R. (2012) A mutant in the *ADH1* gene of *Chlamydomonas reinhardtii* elicits metabolic restructuring during anaerobiosis. *Plant Physiol.* **158,** 1293–1305